AAEC/E590

AAEC/E590

AUSTRALIAN ATOMIC ENERGY COMMISSION

RESEARCH ESTABLISHMENT

LUCAS HEIGHTS RESEARCH LABORATORIES

AN INSTRUMENTED LEACH COLUMN FOR THE STUDY OF SULPHIDE OXIDATION IN WASTE HEAPS

by

R.T. LOWSON

J.V. SARBUTT

MAY 1985

ISBN 0 642 59804 5

AUSTRALIAN ATOMIC ENERGY COMMISSION
RESEARCH ESTABLISHMENT
LUCAS HEIGHTS RESEARCH LABORATORIES

AN INSTRUMENTED LEACH COLUMN FOR THE STUDY OF SULPHIDE OXIDATION IN WASTE HEAPS

by

R.T. LOWSON
J.V. SARBUTT

ABSTRACT

The construction, commissioning and first year of operation of a large-scale, instrumented leach column are described. The column material was sulphidic mine overburden. Monitored parameters included matrix potential, temperature, redox potential, dissolved oxygen, pore space gas, water addition and drainage, together with pH, Cd, Cu, Fe, Ni, Zn, Cl^-, F^-, SO_4^{2-} and PO_4^{3-} in the effluent.

National Library of Australia card number and ISBN 0 642 59804 5

The following descriptors have been selected from the INIS Thesaurus to describe the subject content of this report for information retrieval purposes. For further details please refer to IAEA-INIS-12 (INIS: Manual for Indexing) and IAEA-INIS-13 (INIS: Thesaurus) published in Vienna by the International Atomic Energy Agency.

EXTRACTION COLUMNS; HUMIDITY; LEACHING; LIQUID FLOW; OXYGEN; PROBES; REDOX POTENTIAL; SOLID WASTES; TEMPERATURE MEASUREMENT; THERMOCOUPLES

CONTENTS

1. INTRODUCTION

In work at the AAEC Research Establishment on the oxidation of sulphides in mine waste heaps, a number of assumptions that were made needed to be tested in large-scale leach columns. There are many examples of the use of these columns to evaluate the leachability of ores and waste rocks by natural waters and synthetic leach liquors. The columns range in diameter from a few centimetres to two to three metres, and there is a proportionate variation in height. The majority of columns are operated by pouring liquor in at the top and observing what comes out at the bottom. However, this simple approach provides very little information on processes within the column. To obtain such information a large-scale leach column was constructed; the column was instrumented with probes to detect the redox potential, oxygen concentration, humidity, temperature and water suction, and fitted with access ports for observation, and for gas, liquid and solid sampling. The probes were interfaced with an Apple II computer to allow automatic data logging and analysis. Although automatic data logging is not essential for a single column, several columns will be built, and for multiple columns automatic data logging is essential. The construction, commissioning and first year of operation of this column are described, together with the experience gained with interfacing the various probes to the computer.

2. CONSTRUCTION AND INSTRUMENTATION

2.1 Construction of the Column

The size of the column was determined by the availability of material and the height of the room in which it was to be housed (Figure 1). The column wall and ports were constructed from Vinidex PVC pipe and matching fittings. With the exception of the screwed unions, all the joints were sealed with PVC jointing compound. The column wall was constructed from the largest diameter PVC sewer pipe available. Initially, the pipe was 3 m long × 315 mm o.d. × 298 mm i.d and supplied with a bell end for joining the pipes. The bell end was machined off and saved: the length of the modified pipe was 2850 mm.

Before assembling the column, five suites of ports were made in the column wall. They were evenly separated along the length of the column to produce six sections of rock and an air space at the top. Each suite was labelled as shown in Figure 1. The suites were identical and consisted of three 25 mm i.d., one 15 mm i.d. and four 12 mm i.d. ports.

The 25 mm ports were constructed from modified Vinidex class 18 PVC 25 mm unions (Figure 1, insert a). The union was modified by machining the diameter of the tail of the bolt end to 38.5 mm and the internal flange of the bolt end back by 4 mm to expose the 'O' ring. A 38.5 mm diameter hole was drilled into the column wall, and the bolt end of the union sealed into the hole with PVC jointing compound. The port could be blanked off with a standard Vinidex PVC 25 mm cap. The port could also be used for inspection by inserting a 40 mm diameter Perspex disc in the screwed union. The Perspex disc was sealed onto the exposed 'O' ring.

The 15 mm and 12 mm diameter ports were strengthened by cutting up the bell end into sections 5 cm high by 7 cm across the cord, and cementing them onto the column with PVC jointing compound. A hole was then drilled through the section and the column wall and a short length (about 10 cm) of 12 or 15 mm i.d. PVC electrical conduit inserted (Figure 1, insert b). The joint was sealed with PVC jointing compound. The port could be blanked off with a rubber bung when not in use.

The ports were located spirally along the column to eliminate preferential flow paths. At each level, the ports were evenly spaced around the circumference of the column so that at a given level, the distance between each port was about 123 mm on the circumference, and the distance between each level was about 400 mm.

The 25 mm ports were used for solid or liquid sampling, inspection and accommodating the water suction and humidity probes. The 15 mm ports were used to house oxygen probes, and the 12 mm ports were used for gas sampling and for housing redox potential probes.

The column was supported on a small steel frame to allow access to the base of the column and to compensate for a 1° drainage slope in the floor of the room. The frame, constructed from 25 mm angle iron, was approximately 360 mm^3.

The column stood on a base plate placed on the steel frame. The base plate was made from core board, and measured 450 mm^2 × 35 mm thick. A 34 mm diameter hole was drilled through the centre of the base plate to accommodate a short length of 34 mm o.d, 30 mm i.d. PVC pipe which acted as a drain. A circular slot 5 mm deep, 296 mm i.d. and 318 mm o.d. was milled into the base plate to accommodate the column wall. The base plate was covered with 0.5 mm thick PVC sheet; a hole was pierced in the centre and the edges glued to the inside of the drain with PVC jointing compound. A spacer was made from a standard Vinidex class 18 PVC 155 mm union, the length of which was reduced to 10 cm and the edges crenellated at each end. The spacer was placed slightly off centre on top of the base plate. A retaining plate, 296 mm in diameter, was made from 12 mm thick Perspex sheet. The retaining plate was drilled with many 10 mm diameter holes in a fairly random pattern and placed on top of the spacer. The column wall was mounted onto the base plate so that it seated in the base plate slot; it was then sealed into position with PVC jointing compound.

A standard Vinidex class 18 PVC 25 mm union was attached to the drain which was then closed with a short length of PVC pipe and a cap; the cap was pierced by a 5 mm diameter hole into which was inserted and sealed a length of plastic tubing, bent to form a water trap and syphon to which was attached a collection flask. A 12 mm thick Perspex lid, in which was drilled a 5 mm diameter hole for water addition, was clamped to the top of the column.

The material to be tested was sulphidic overburden supplied by Woodlawn Mines Pty Ltd, NSW. This material was a friable dry soil with a fair quantity of fines and a few large boulders. Gross material was removed with a 25 mm sieve and the remaining material was used in the as-received condition.

A piece of cotton fabric was placed on the retaining plate to stop the fines from falling through. The column was packed by lowering small buckets of material into it. The material was tamped into place with a thick piece of wood. As each instrument probe level was reached, a set of three thermocouples, a redox probe and the ceramic cup of a tensiometer were packed into the column. Care was taken to ensure that the ceramic cup was not packed with predominantly coarse material. A Wettex absorbent cloth was placed on top of the material to disperse the water as it was added to the column.

The rock density of the material was found by boiling a known weight of rock with a measured amount of water, then determining the excess volume of water after the rock had settled in a measuring cylinder. It was necessary to boil the rock to remove the last vestiges of entrapped air [N. Collis-George 1983, private communication]. For a 2 kg sample, a 1 per cent swelling of the rock was observed, and the rock density was 2.599 g cm^{-3}, which is typical for this type of material. The column was filled with 296 kg of material, which occupied 0.162 m^3, giving a packed density of 1.83 g cm^{-3} and a pore volume of 47.9 L.

2.2 Temperature

2.2.1 Temperature detectors

The temperature was expected to vary over the range 15°C (lowest ambient) to 80°C (highest reported temperature for a bacterially catalysed reaction). The following factors were taken into account when choosing the appropriate detector:

(i) Linear response within the selected range.

(ii) Output to be an analogue electrical signal.

(iii) Absence of hysteresis.

(iv) Sturdy construction and corrosion resistant.

(v) Minimal effect as a heat sink.

(vi) Minimal heat input.

(vii) Small.

(viii) Inexpensive.

(ix) Replaceable.

Two types of detector were considered: the semiconductor temperature transducer AD590 and the thermocouple.

The semiconductor temperature transducer, AD590, was described in detail by Timko [1976]. It is supplied commercially as a monolithic integrated circuit incorporating all the necessary detection and amplification electronics. With supply voltages between 4 and 30 V, the device has a linear current output of 1 μA K^{-1} and is calibrated to 298.2 μA at 298.2 K by laser trimming the thin film resistors within the chip. The device eliminates the need for linearisation circuitry, precision voltage amplifiers, resistance measuring circuitry and cold junction compensation. It has an output impedance of >10 MΩ which provides a good rejection of supply voltage drift and ripple, and makes the device insensitive to voltage drops over long lines.

Unfortunately, the combination of the AD590 with an Apple analogue-to-digital converter (ADC) board significantly reduces the overall sensitivity. In addition, the transducer will also heat the column. The nominal output current is 300 μA at 300 K (ambient temperature). With a supply of 10 V, the transducer operates at 3 mW, hence with three transducers per level the column would receive about 10 mW at each level. As the average column volume between each level is 0.0275 m^3, the heat input from the temperature detectors would be around 0.1 W m^{-3}. The maximum and minimum observed heat densities in the White's overburden heap at the abandoned Rum Jungle mine site (Northern Territory, Australia) were 1 and 0.2 W m^{-3} respectively [Harries and Ritchie 1981]. Consequently, the transducers would supply heat to the column in quantities commensurate with that being observed in waste heaps. Accordingly, use of this type of detector would require a voltage subtraction circuit to improve overall sensitivity, and software and hardware switching to turn the device on and off.

The preferred detector was the chromel-alumel thermocouple which is supplied in a 1 m long, 3.125 mm diameter stainless steel sheath in which the thermocouple is insulated with magnesium oxide. The cold end was pot-sealed into the sheath and colour-coded according to British Standard B.S. 1827. The thermocouples were connected to the computer interface using chromel-alumel compensated leads.

The chromel-alumel thermocouple has a near-linear electrical response and a temperature coefficient of 40 μV °C^{-1}. This response had to be amplified to about 10 mV °C^{-1}. The general requirements of a thermocouple amplifier are that it should have low offset voltage drift, good gain accuracy, low noise and cold junction compensation. The selected circuit [NSC 1980] reproduced in Figure 2, is basically a non-inverting amplifier with the gain set to give an output of 10 mV °C^{-1}. It uses a supermatched transistor pair, supplied as the monolithic unit LM 194, as an input stage differential amplifier to ensure an offset voltage drift of less than 0.1 μV °C^{-1}, a current gain matched to 2 per cent, a common mode rejection of >120 dB, and very low noise. The output stage is a non-inverting low gain operational amplifier with the gain set to give an output of 10 mV °C^{-1}. The output sensitivity is arbitrary and can be set higher or lower. Cold-junction compensation is achieved by deliberately unbalancing the collector currents of the LM 194 so that the input offset voltage drift just equals the thermocouple output at room temperature. This technique requires the LM 194 to be at the same temperature as the thermocouple cold junction, so the thermocouple leads should be terminated as close as possible to the LM 194.

The deliberate offset voltage created across the LM 194 input must be subtracted with an external reference voltage. This is achieved by combining the zener LM 129 and resistance network R1 to R6 so that, for an arbitrarily selected temperature T1, the gain adjustment has no effect on the zero adjustment. This simplifies the calibration procedure. The correct values for the resistances are determined from the following design equations, in descending order of use. The worked examples are for a 10 mV °C^{-1} output with a chromel-alumel thermocouple. Select

$$R9 = 300\ k\Omega \pm 1\%$$

$$R10 = R9.e^{-\alpha(1.16 \times 10^4)} = 191\ k\Omega \pm 1\%$$

where α is the thermocouple output in μV °C^{-1} and, for chromel-alumel, is 40 μV °C^{-1};

$$R8 = 200\ k\Omega$$

Select R4 in the range 50 to 250 kΩ, in this case 250 kΩ:

$$R5 = \frac{(R4)(T_1)(\alpha)}{S(T_1 - T_0) - (T_1)} = 13\ k\Omega$$

where T_1 is the temperature in K at which the gain adjustment is independent of the zero adjustment (and in this case is 298 K); T_0 is the equivalent temperature in K for the zero of the selected temperature scale (in this case 0°C); and S is the output scale factor (in this case 0.01 V °C^{-1});

$$R2 = \frac{(R4)(R5)(1-E^*/100)}{(S-\alpha)[R5-((R4)/S-\alpha)]} = 1.06\ k\Omega$$

where E* is the permitted gain error and is set at 2.5%;

$$R1 = \frac{(R2)V_z - \alpha(T_1)(0.95)}{\alpha(T_1)} = 590\ k\Omega$$

where V_z is the zener reference voltage;

$$R3 = \frac{(E^*)(R2)}{50} = 50\ k\Omega$$

$$R7 = (R9/R10)(R2) = 1.6\ k\Omega$$

$$R6 = R1/10 = 50\ k\Omega$$

The interface may be calibrated as follows:

(i) Place the thermocouple in an environment which is at temperature T_1. In the above calculations T_1 was at room temperature; however it could be any selected temperature such as that of ice, a thermostatted oven, hot water, etc. Adjust R6 to give a suitable output which may be O V or any selected value.

(ii) Place the thermocouple in an environment which is at temperature T_2; this may be greater or less than T_1 . Adjust R3 to give the selected gain which, in this case, is 10 mV $°C^{-1}$.

(iii) Return the thermocouple to room temperature and short-circuit the thermocouple and D1 to ground. Adjust R11 to give a proper output at room temperature (in K). For 10 mV $°C^{-1}$ this is 2.98 at an ambient temperature of 25°C. Remove short-circuits and, if necessary, re-adjust R6 to zero output.

Steps (iii) and (iv) are unnecessary if exact cold-junction compensation is not required; R11 is simply shorted out and compensation will be within ±5% without adjustment.

All resistors except R8 and R9 should be the 1 per cent metal film type for low thermocouple effects and have low temperature coefficients. R9 and R10 should track to 10 ppm $°C^{-1}$, R3, R6, and R11 should have a temperature coefficient higher than 250 ppm $°C^{-1}$, and R1, R2 and R4 should track to 20 ppm $°C^{-1}$. Capacitor C2 is added to reduce spikes and noise from long thermocouple lines.

The input impedance of this circuit is >100 MΩ , so high thermocouple impedance does not affect the scale factor. Zero shift due to input bias current is approximately 1 °C for each 400 Ω of lead resistance with a 40 μV $°C^{-1}$ chromel-alumel thermocouple.

Non-linearity of the thermocouple over the required temperature range is negligible and within the measuring error, consequently no provision was made for this effect. The effect can be compensated for by replacing R4 with resistor/diode networks or by software programming.

2.2.2 Temperature calibration

After assembly of the complete thermocouple system, the circuit should be checked for high frequency oscillation (around 1 MHz) at the pins on the ADC board. This noise can be due to inadequate compensation at the 'op-amps' circuit, *i.e.* the value for C1 is too low, or use of excessive lengths of flat ribbon cable (a maximum length of 2 m is recommended). Noise should be less than 10 mV peak to peak.

It is advisable to calibrate the thermocouples and interface boards after assembling the complete system, using software to read the voltage on the visual display unit. If the thermocouples and interface boards are calibrated without the computer, using a digital voltmeter, there may be errors due to voltage drops at the ADC board. A digital voltmeter will smooth 1 MHz frequency noise, whereas the noise will be observed on the visual display unit as a random valued result because the analogue signal is read at the ADC board at a frequency similar to that of the noise.

2.3 Dissolved Oxygen

Dissolved oxygen was measured at each level by placing a dissolved oxygen probe in contact with the moist solid. The probe was a Johnson lead/silver cell with an output of 0 to 30 μA across the range 0 to

100 per cent O_2 saturation. The cell was designed and manufactured at the AAEC Research Establishment, and is shown in detail in Figure 3. The cell was constructed from glass and housed in a corrosion-resistant titanium guard which fitted into the 15 mm ports of the column. The titanium guard was made from hexagonal bar titanium, 20 mm across the flats and 18 cm long. The main section of the bar was machined to a sliding fit into the 15 mm port. A short length of 11/16" B.S.W. thread was machined close to one end which was then finished off with a short length of the original hexagonal section. The inside of the bar was machined to a sliding fit over the glass cell. A small internal recess was machined at the outer end of the guard so that the cell could be sealed into it with caulking compound.

The glass cell was a tube 22 cm long and 11 mm in diameter. Approximately 8 mm of the sensor end was narrowed to about 8 mm diameter. At the top end, a short length of 6 mm diameter tubing was attached off-centre (see Figure 3). A B5/13 ground glass socket was attached at right angles just below the top of the cell and on the same side as the off-centred tubing.

The silver electrode was a flat coil of 0.5 mm diameter silver wire. The diameter of the coil was slightly less than the outside diameter of the sensor end of the glass cell. The centre of the coil was finished with a 5 mm length of wire projecting from the cell, as shown in Figure 3. A colour-coded, Teflon-coated copper lead was soldered onto the coil. The joint was insulated by painting it with Perspex glue and then covering it with shrink tube. A 2 mm thick inert spacer made from nylon gauze was threaded onto the lead and pulled close to the silver coil.

The high purity lead electrode was made from lead shot rolled into 0.4 mm thick sheet from which was cut a 1 x 2 cm rectangle. A colour-coded Teflon-coated copper lead was soldered onto one side. The lead sheet was then rolled into a split tube with a diameter slightly less than the internal diameter of the sensor end of the cell. The soldered joint was insulated by painting it thoroughly with Perspex glue.

The probe was assembled by passing the electrode leads through the sensor end and out through the top of the cell. The lead electrode was inserted and positioned just above the narrowed sensor end. The silver electrode assembly was then emplaced so that the coil lay across the sensor end which was then covered with a membrane made from 0.005" Teflon sheet. The membrane was held in place over the sensor tip by a tight-fitting ring cut from PVC tubing. Care was taken not to tear the membrane. The top end of the probe was sealed with Araldite epoxy glue.

An electrolyte solution of 5 *M* acetic acid, 0.5 *M* sodium acetate and 0.1 *M* lead acetate was prepared and boiled to remove all dissolved air. The cell was completely filled with electrolyte and the cell then closed with a ground glass stopper.

The circuit for interfacing the oxygen probe with the computer, shown in Figure 4, is basically a current-voltage converter. The probe current is dropped across resistances R1 and R5 with R5 variable to allow adjustment for variable source impedance. C1 was included as a decoupling capacitor. The output voltage from the resistance network was amplified by a high gain non-inverting amplifier circuit using a 741 series op-amp. This particular op-amp is protected against short-circuit and has no 'latch-up' problem. For a non-inverting configuration, the gain is given by 1 + (R2+R4)/R6 and is adjusted by R4. R3 is a zero adjustment using the offset null facility of the op-amp.

2.4 Redox

The redox probes were rectangular sheets of 0.1 mm thick platinum welded to 15 cm long by 0.8 mm diameter platinum wire leads. The probes were embedded into the column material as the column was built.

The redox potential was measured with reference to a calomel electrode located outside the column and level with the base plate, which was also the saturation point or water table for the column. The calomel electrode assembly is illustrated in Figure 5. The electrode holder was made from an 8 cm long by 2 cm o.d. glass tube, the top end of which was finished with a B14 ground glass socket. A short side arm of 5 mm o.d. glass tube was attached to the holder just below the ground glass socket and another of similar dimension was attached to the holder just above the base. About 20 cm of PVC tubing was attached to the lower side tube and the other end was attached to a small glass funnel which could be raised or lowered.

above the base plate. A fibre-filled glass tube was sealed into the hole and connected to the top side arm of the holder by a short length of PVC tubing. The electrode was a commercially available Jena type B351 calomel electrode with a B14 ground glass cone fitting. The assembly was filled with the solution that had drained from the column and the height of the funnel adjusted so that the electrode holder did not quite overflow. The electrode was then inserted into the column and connected to the recording instruments.

Initially the potential was measured with a digital voltmeter. Subsequently, an interface was built to allow the readings to be recorded by the computer. The interface shown in Figure 6 is basically a non-inverting low gain amplifier which provides good impedance matching with the ADC card of the computer. By including a variable gain adjustment, all 128 channels of the positive or negative side of the ADC board can be used. Since the input will be within the range 0 to ± 1 V, the gain may be adjusted to better than one channel per 10 mV input.

2.5 Humidity

The humidity was measured with a Phys-Chemical Research Corporation Humeter Model B humidity meter equipped with a five-position switch box and a set of five PCRC-11 HPB probes. These particular probes included an AD590F temperature sensor (see Section 2.2.1). The instrument response was 0 to 100 per cent relative humidity in the temperature range -5 to 75 °C. In a closed system, the response time for a 63 per cent change in relative humidity is 30 s and, for the same percentage change in temperature, it is less than 30 s. Hysteresis by the temperature sensor is minimal, and that by the humidity sensor is caused, in part, by adsorption and desorption. For a change in relative humidity from zero to 100 per cent and back to zero, there is a narrow hysteresis loop that is widest at 50 per cent relative humidity, with a width in the region of ± 2.5 per cent relative humidity. Smaller humidity fluctuations fall within this hysteresis loop. The instrument and probes were calibrated by the manufacturer.

The probes were mounted in the 25 mm ports and pressed against the face of the column material. All the gaps between the probes and the ports, and probe cable exits, were sealed with silicone caulking compound.

2.6 Water Potential

Water potential is formally defined as the amount of work that a unit quantity of water in an equilibrium soil-water system is capable of doing when it moves to a pool of water in the reference state at the same temperature. The reference state must be specified in terms of position and composition [Hanks and Asheroft 1980]. In the present study, the reference level was the free draining base of the column and the reference concentration was the same as that of the column solution.

Water potential is the sum of a number of component potentials given by

$$U_w = U_g + U_p + U_s + U_m$$

where U_w is the water potential, U_g is the gravitational potential, U_p is the pressure potential, U_s is the solute potential, and U_m is the matric potential (defined in Section 2.6.4).

2.6.1 Units

The water potential may be expressed as work per unit mass, work per unit weight or work per unit volume. This has resulted in a plethora of units for expressing water potential; the conversion factors for some of these are given in Table 1.

UNITS FOR WATER POTENTIAL

Unit	Conversion Factor (to bars)	Expressed as
Bars	1	work per unit volume
Atmospheres	0.9869	work per unit volume
kPa	100	work per unit volume
dynes·cm^{-2}	1×10^6	work per unit volume
cm of H_2O	1020	work per unit weight
cm of Hg	75.01	work per unit weight
J kg^{-1}	100	work per unit mass
erg g^{-1}	1×10^6	work per unit mass

2.6.2 Gravitational potential

The gravitational potential (U_g) is the potential work involved in transfering a unit mass of water from a given point to the reference point; work W is given by

$$W = pVgh$$

where p is the density, V is the volume, g is the gravitational constant, and h is the difference in vertical height between the two points. The gravitational potential may be expressed as work per unit mass,

$$U_g = W/pV \quad = gH \quad (J\ g^{-1})$$

work per unit weight

$$U_g = W/pVg \quad = h \quad (cm\ of\ water)$$

or work per unit volume,

$$U_g = W/V \quad = pgh \quad (Pa)$$

The gravitational potential is usually measured as a difference in height , that is as work per unit weight. Conversion to work per unit mass or work per unit volume requires multiplication by the appropriate conversion factors for g (9.796 m s^{-1}) or pg.

2.6.3 Pressure potential

Pressure potential (U_p), also known as submergence potential, piezometric head and piezometric potential, is the potential for work through the submergence of a given point below the water surface or water table. The equations and units are identical to those for gravitational potential except that h is now the distance between the point and the water surface. For the present work, the water surface or water table was located at the free-draining base of the column, which is also the reference point.

2.6.4 Matric potential

The matric potential (U_m) is produced by the adsorptive forces of surface tension and surface adsorption by the soil matrix (hence 'matric'). It is observed as water suction by the soil and is measured by contacting a captive volume of water with the soil through an inactive porous membrane. The captive volume is attached to a manometer or other pressure indicator and the degree of suction observed. The total system is termed a tensiometer.

The matric potential of the column was measured at each level by installing a ceramic bulb as the porous membrane in the soil and attaching it to one limb of a mercury manometer *via* lengths of glass tubing (see Figures 7 a-c).

The ceramic bulbs, supplied as 'Hydratal 1000 *standard cups*', were 2.3 cm o.d. by 7 cm in length. Each cup was closed at one end with a rubber seal having a central hole for attaching to a manometer. The sections of glass tubing from the ceramic cup were joined by short lengths of plastic tube to give flexibility. Long lengths of plastic tubing should be avoided because the degree of gas diffusion through the tube walls then becomes unacceptably large. A tee piece fitted with a glass tap was attached to the highest point of the closed limb to allow the limb and cup to be filled with water and purged of gas.

The manometer reading is the water suction at the mean centre-line of the porous membrane. The observed value must be corrected for the unbalanced length of water column between the closed manometer limb and the centre-line of the porous membrane. There are three typical cases, which are shown in Figures 7 a-c.

Case 'a' is for the ceramic cup placed well above the centre-line of the manometer so that there is an apparent pressure due to the excess pressure of the water column. Case 'b' is for the ceramic cup placed above but close to the centre-line of the manometer, so that the observed suction is less than the real suction because of the pressure of the water column. Case 'c' is for the ceramic cup placed below the centre-line of the mercury manometer and the observed suction is enhanced by the suction of the water column.

The suction is measured as the difference, h_m, in height between the open, h_o, and closed, h_c, mercury manometer limbs:

$$h_m = h_o - h_c$$

The sign must be included in the reading. If the difference in height between the centre-line of the porous membrane and the centre-line, or zero point, of the manometer is designated h_z and the height of the unbalanced length of the water column in the closed limb h_w, then the value for h_z is positive when the centre-line of the ceramic cup is above the zero of the manometer, and negative when it is below. As long as the sign is included in the values for h_m, h_w and h_z, the suction is given by the general equation

$$\begin{aligned} U_m &= h_m(\rho_m/\rho) - h_w \\ &= h_m(\rho_m/\rho) - (h_z + \frac{1}{2}h_m) \ (cm \ of \ water) \end{aligned}$$

where ρ_m is the density for mercury and ρ is the density for water. The matric potential can be expressed in terms of work per unit mass and work per unit volume when multiplied by the appropriate factors.

Ceramic cup tensiometers have two limitations. The first is that the probe has a slow response, but this did not cause any significant error in the present application. The second limitation is that at high suction the soil gas penetrates the ceramic cup causing the water column in the tensiometer to break. Gas penetration is due partly to the high chemical gradient for the gas across the ceramic cup at high suction and partly to the significant pressure gradient developed across the height of the ceramic cup. The latter restriction limits the method to a maximum suction of 70 cm Hg (0.9 atm, 0.9 bars, 90 kPa).

2.6.5 Hydraulic potential

In the absence of a semi-permeable membrane, the solute component of water potential is essentially zero. The summation of the remaining terms is commonly known as the hydraulic potential (U_h) :

$$U_h = U_g + U_p + U_m$$

Under equilibrium conditions, the hydraulic potential is constant. When quoting values for the hydraulic potential, it is necessary to state the reference level. Two commonly used reference levels are the ground surface and the water table; in the present study the latter was chosen. Under flow conditions, the hydraulic potential will be a function of depth.

2.7 Solution Analysis

The effluent was analysed for pH using a Radiometer PHM 84 pH meter with Jena type N61 combination pH electrodes. The heavy metals cadmium, copper, iron, nickel and zinc were analysed with a Varian 975 atomic adsorption spectrophotometer. The chloride, fluoride, phosphate and sulphate anions were analysed by anion chromatography using a Dionex Autolon System 12 analyser.

2.8 Gas Analysis

The pore space gas was analysed by withdrawing a gas sample with a hypodermic syringe inserted through a septum on a 12 mm port. The sample was immediately analysed on a Shimadzu GT8AP gas chromatograph using a 6 m 'Porapac R' column, and helium as carrier gas, and a thermal conductivity detector.

3. RESULTS

3.1 Temperature

The temperature inside the column remained at 20 ± 1°C throughout the year. The temperature was occasionally checked by inserting mercury-in-glass thermometers into the column. The results agreed with the data displayed from the computer.

3.2 Dissolved Oxygen

No dissolved oxygen results were obtained during the first year of operation.

3.3 Redox Potential

The redox potential is plotted in Figure 8, with reference to the saturated calomel electrode (SCE) at each level as a function of time. The redox potential was independent of position in the column and produced similar fluctuating patterns with time at each level. Over the period of 200 days, the average initial value of 0.625 V for the five levels rose to 0.675 V and then dropped to 0.65 V.

3.4 Humidity

Humidity probes were installed 308 days after start-up. The readings rose rapidly to about 80 per cent relative humidity. Results over the next few days were contradictory; the fault was traced to inadequate seals. After resealing with silicone caulking compound, the relative humidity rose to between 99 and 100 per cent, where it has since remained.

3.5 Water Addition and Matric Pressure

The column was commissioned on 2 June 1982. Water addition was to be commensurate with typical rainfall rates, but such rainfall rates are rather difficult to define. The median annual rainfall at Sydney is 1206 mm with an annual evaporation of 1018 mm, and the rainfall is spread over the year with a higher rate in the summer than in the winter [Dulley 1982]. The median annual rainfall at Darwin is 1548 mm [Bureau of Meteorology 1968] with an annual evaporation of 2400 mm [Davy 1975]; however, it is restricted to the six months of the wet season. Thus the average daily rainfall in Sydney is 3.3 mm d^{-1} for the whole year whereas in Darwin it is 8.4 mm d^{-1} during the wet season and zero during the dry season.

There are two further complications in determining a typical rainfall rate. The leach column was designed for zero evaporation whereas, in the natural environment, evaporation from a heap may be anything from 33 to 100 per cent of the rainfall. Further, the column was also designed for total infiltration whereas, in the natural environment, run-off to infiltration is usually within the ratio 2:1 and 1:2, depending on the physical constraints of the receiving surface [Daniel *et al.* 1982].

The rate of water addition was set at 50 mL d^{-1} as a batch addition; this corresponded to a rainfall rate of 0.7 mm d^{-1} with total infiltration and zero evaporation. This rate was considered to be commensurate with the natural rainfall, taking normal evaporation and infiltration effects into account.

After 30 days, it became clear that the wetting front would take about one year to pass through the column. Accordingly, the addition rate was increased to wet the column more rapidly without causing flooding at the top. For the next 50 days, the rate of addition was increased to 100 mL d^{-1} as a batch addition; this was still too slow, so the rate was increased to 500 mL d^{-1} by batch addition. Under these conditions, the wetting front travelled fairly rapidly down the length of the column as was seen from the matric suction readings. The matric pressure readings indicated the likelihood that the surface had become saturated. Ponding on the surface was not observed.

Drainage from the base of the column started 118 days after commissioning. The batch addition of water to the top of the column was immediately cut back to 50 mL d^{-1} and has since remained at this rate. Total addition and total drainage are plotted as a function of time in Figure 9, which also has an insert showing the total drainage for the first 25 days of drainage.

Within two days, the drainage rate rose to 500 mL d^{-1}, that is it was the same as the rate of addition before drainage occurred. The drainage rate then slowly decreased and by day 25 had dropped to just less than 50 mL d^{-1}. The column appears to have a time-lag which is a function of the condition of the column, the flux and the length.

Once the steady-state flow had been achieved, the addition rate was maintained at 50 mL d^{-1}; however, the drainage rate dropped to 36 mL d^{-1}.

The matric pressures at each level are plotted as a function of time in Figure 10. The column was effectively dry before commissioning and the addition of water to the top of the column caused a wetting front to pass down its length. Before the arrival of the wetting front, the soil had a suction greater than 8000 mm of water. The actual suction under these conditions was never measured because under high suction the tensiometers broke down, letting air into the closed limb of the manometer. As the wetting front passed each level, the tensiometer stabilised to a low suction in the range 100 to 300 mm of water, depending on the relative level of the tensiometer.

When the addition rate was cut back to 50 mL d^{-1}, the suction on the tensiometers changed over a period of 30 to 40 days to a steady value. The period taken for this change was the same for all the tensiometers, *i.e.* it was independent of depth and time. At day 200 the suction on tensiometers E,D,C and B increased in the expected order for the system. Tensiometers E and D were particularly stable, whereas C and B fluctuated in phase with each other. Tensiometer A developed an anomalously low reading and remained at that value for 350 days. Consequently, the tensiometer was flushed out and recharged An equilibrium reading was achieved within an hour, but the value was still very low.

After day 220, the suction on tensiometer B started to drop. This drop then started to occur in tensiometers C, D and E. The onset of the change was qualitatively a function of time, which may be interpreted as being a function of depth. The suction was still dropping at the end of the first year of operation.

3.6 Solution Analysis

The effluent was analysed for pH, the heavy metals cadmium, copper, iron, nickel and zinc by atomic adsorption spectroscopy, and the chloride, fluoride, phosphate and sulphate anions by anion chromatography. The results are plotted in Figure 11.

3.6.1 pH

Between day 118 and day 180 the pH remained reasonably steady at 3.6 ± 0.1. During this period, the matric pressure was developed to maximum suction. From about day 180, the pH declined steadily and, by day 260, reached 2.85. There appears to be a pH step between day 180 and day 240 which may have been due to the use of an incorrect buffer for the calibration of the pH meter.

3.6.2 Heavy metals

Once a steady-state flow condition had been achieved, the cadmium, copper, nickel and zinc levels stabilised:

Element	mg L^{-1}
Cd	78 ± 4
Cu	7.2 ± 0.2
Ni	94 ± 4
Zn	19 ± 1

and there were common local peaks and dips in the plots for these metals and for the sulphate concentration.

In contrast, the plot for iron was independent of the other metals and anions. At the onset of drainage,the iron concentration was about 200 mg L^{-1}; however, as the rate of flow decreased, this concentration dropped by a factor of ten, stabilising at 30 ± 2 mg L^{-1}. Unfortunately, the ferrous and ferric ratios were not determined.

3.6.3 Anions

The chloride, fluoride and phosphate anion concentrations were low and constant;

Anion	g L^{-1}
Cl^-	0.2 ± 0.1
F^-	0.2 ± 0.1
PO_4^{3-}	1.0 ± 0.2

In comparison, there was a high sulphate concentration which initially fluctuated in phase with the varying heavy metal concentrations and then settled down to a steady value of about 78 ± 2 g L^{-1}.

3.7 Gas Analysis

No gas analyses were carried out during the first year of operation.

4. DISCUSSION

4.1 Construction of the Column

The construction of the column posed no major problems and the basic design and materials were quite suitable for this type of work. Two modifications will be introduced into future columns (i) to improve the seal between the column wall and the plastic sheet, and (ii) to reduce the volume between the retaining plate and drain.

Initially, the performance of the seal between the base of the column wall and the plastic sheet was satisfactory. However, once drainage had settled to a steady rate, an artificial water table was imposed on the column by raising the drain syphon above the base of the column. The seal then failed, but whether the failure was at the column wall or at the drain is not clear. The seal was repaired by draining the space below the retaining plate and then flooding the internal surface of the base plate with Aquadhere PVA glue. Since, by this stage, the column appeared to be generating its own water table, no further attempts were made to impose an artificial one. A commercial PVC flange is adequate to seal the base and this will be used on future columns in place of the plastic sheet.

In the present design, the volume below the retaining plate is about five litres. For normal drainage, the size of this space is of no consequence. However, in cases where an artificial water table using the column solution is required, this bottom space must be kept to a minimum. The combination of a PVC flange and a modified retaining plate will eliminate the need for the spacer and overcome the problem.

4.2 Temperature

The column failed to heat up because the system sustains a higher heat loss than a waste dump. A possible solution is to use a jacketed column in which the interwall space is either evacuated or filled with a recirculated fluid. This will be investigated on a second column.

The poor effective sensitivity of the total measuring system (2.5 °C per channel) will have to be improved. The source of the problem is that the ADC board is limited to the range 0 to +5 V and 128 channels or 39 mV per channel. Effective sensitivity, *i.e.* the sensitivity of the value shown on the visual display screen, is at a maximum when all the channels are employed for the total temperature range. Thus 0 V, channel 0 is the minimum expected temperature and 5 V, channel 128 is the maximum. However the probe, either as a thermocouple or as an AD590 device, will have a voltage at the minimum expected temperature which will be amplified by the interface board; hence it will be necessary to back-off this initial voltage with a zener diode and resistance network to reduce the output from the interface to zero at the minimum temperature. This facility is already available on the thermocouple interface board but needs to be designed into the AD590 board. To achieve 5 V output at the maximum expected temperature, a variable gain potentiometer will be added to the interface board.

4.3 Redox Potential

The redox potential was independent of position in the column and did not vary significantly with time. The common fluctuation was attributed to variations in the liquid junction potential of the salt bridge of the reference calomel electrode. Improved stability could be achieved by draining the column directly from the water table. This solution could then be used in a double-flow liquid junction in which the two flows are separated by a porous disc. This device would maintain electrical contact between the column solution and the reference electrode and also maintain mass balance for the draining solution.

The redox potential was about 0.65 V (SCE), that is 0.41 V (SHE). This mixed potential is the sum of the dominant oxidising and reducing reactions which are occurring in the solution. The chemical results

indicate that the redox potential is dominated by zinc and copper redox couples. The Cu-S and Zn-S Eh-pH diagrams [Peters 1976] indicate that it would be difficult to identify the dominating redox couple from the potential and pH readings for such a complex system. The conditions are favourable for the precipitation of jarosite $KFe_3(SO_4)_2(OH)_2$ [Lowson 1982]. This material acts as an electrochemical buffer and, as a solid, it will tend to block the pore space.

4.4 Humidity

For a pure water system, the relative humidity should be 100 per cent in the pore space. However, as ions are introduced into the solution and the solution concentrates there is a small depression of the volatility according to Raoult's law. Present operating conditions indicate that the depression of the vapour pressure in the pore space is below the sensitivity of the detectors which, in the region of 100 per cent relative humidity, is unknown. Fluctuations of two per cent could be attributed to local weather conditions. It is hoped that the readings will settle down once the room in which the column is housed is air-conditioned to a constant temperature, and when the column is operated in a less saturated state.

4.5 Water Addition and Matric Pressure

The total water balance is plotted in Figure 9 with the assumption that evaporation and leakage terms are insignificant. At the commencement of drainage, the column contained 28.4 L of water. This dropped to 24 L within 30 days, but rose again to 27 L, which was about 50 per cent of the pore volume by the end of the first year of operation and continues to rise. It may be concluded that the column has not yet reached a steady-state condition.

The matric and hydraulic pressures are plotted in Figure 12 as a function of depth for the following times:

(i) 120 days - the start of drainage,

(ii) 200 days - the stable matric pressure regime, and

(iii) 350 days - one year's operation.

The matric pressure at the top of the column was not measured. For short periods during water addition, the matric pressure was zero owing to flooding. However, continuous ponding on the surface was not observed.

The 120-day graph is the result expected for a flowing system with regular water addition at the surface and a free-draining base. The 200-day plot is unusual. The very low suction at level A suggests near-saturation conditions or a faulty probe. The suction at levels B, C and D is in the region expected for an undersaturated soil. However, the hydraulic pressure at level E is negative. This may be because the water table had risen above the base of the column. Under such conditions a submergence pressure term should be included in the summation for hydraulic pressure so that the hydraulic pressure remains zero at the reference point. The 350-day graph lends weight to this argument. The matric pressure at levels B, C and D has been reduced, indicating that the water content of the column increased and the hydraulic pressure at the base became more negative.

For a column in steady-state equilibrium, the flux is related to the hydraulic pressure by Darcy's law:

$$J = -K \frac{dU_h}{dx}$$

where x is the distance down the length of the column. For a column area of 0.0697 m^3, the input flux at 50 mL d^{-1} addition was 8.303 x 10^{-9} m s^{-1} whereas the drainage flux at 36 mL d^{-1} drainage was 5.978 x 10^{-9} m s^{-1}. The hydraulic gradients at the top and bottom of the column were determined from Figure 12 as the mean slope between the surface and the top two levels, and the base and the bottom two levels, respectively, and the following values (Table 2) were determined for the hydraulic conductivity:

TABLE 2
HYDRAULIC CONDUCTIVITY OF COLUMN

Position	Time (d)	Flux ($m\ s^{-1}$)	Hydraulic Gradient ($mm\ mm^{-1}$)	Hydraulic Conductivity ($m\ s^{-1} \times 10^{-9}$)
Top	120	8.303×10^{-9}	1.36	6.10
	200	"	2.33	3.57
	350	"	1.66	5.0
Base	120	5.978×10^{-9}	0.69	8.68
	200	"	0.50	11.9
	350	"	0.81	6.75

The results are somewhat anomalous, since the change in hydraulic conductivity at the top of the column with time is the inverse of the change at the bottom. At this stage the cause of this is not clear, but it is noted that the water content of the column is continuing to increase, and that the column may be undergoing physical changes owing to the production of insoluble products such as jarosite which expand into and block the conducting pores.

4.6 Solution Analysis

The cadmium, copper, nickel and zinc concentrations fluctuated in phase and then settled down to steady concentrations. The fluctuations were probably caused by some instability within the column and disappeared as the column started to leach. A feature missing from most of the graphs is a very high initial concentration of soluble ions caused by the flushing of precipitated salts from the column. This indicates that the material had not started to oxidise or revert to a soluble form before leaching.

The exception is the graph for iron. The concentration for this ion was initially high, but it then dropped rapidly by a factor of ten to a relatively low and steady value. The variation in iron concentration may have been due to a number of factors, including change in liquid flow rate, change in the amount of available oxygen, onset of bacterial catalysis, and precipitation of iron products such as jarosite. It is unfortunate that the ferrous to ferric ratio was not measured. In future columns, this ratio will be measured as the liquid drains off the column.

The chloride, fluoride and phosphate anion concentrations remained low and steady. The sulphate concentration fluctuated in phase with the heavy metals due to the common source being sulphide.

After an initial steady value, the pH slowly dropped from 3.6 to 2.8. This drop appears to be independent of any other cation or anion, flow rate or matric pressure and is an indication of changing chemistry within the column either because of the onset of bacterial catalysis or through the formation of product buffers such as jarosite. Identification of the mechanism requires solid sampling at the water table. This may be attempted during the next year of operation.

5. ACKNOWLEDGEMENT

The authors wish to acknowledge the advice of the late Dr. Tom Babij of New South Wales University on the construction of the oxygen probe and interface board.

6. REFERENCES

Bureau of Meteorology [1968] - Review of Australia's Water Resources, Monthly Rainfall and Evaporation. Bureau of Meteorology. The Australian Water Resources Council, Melbourne.

Daniel, J.A., Harries, J.R. and Ritchie, A.I.M. [1982] - Runoff and seepage from waste rock dumps containing pyritic material. Proc. *Hydrology and Water Resources Symposium*. Melbourne, 11-13 May, Inst.. Eng., Aust.

Davy, D.R. [1975] - The pollution cycle at Rum Jungle - controlling factors, basic mechanisms and degree. In *Rum Jungle Environmental Studies*, Chapter 3. AAEC/E365.

Dulley, J.E. [1982] - New South Wales Year Book, Number 67. Australian Bureau of Statistics, Sydney.

Hanks, R.J. and Ashcroft, G.L. [1980] - Applied Soil Physics. Unit 2 : Water Potentials. Springer-Verlag, New York.

Harries, J.R. and Ritchie, A.I.M. [1980] - The use of temperature profiles to estimate the pyritic oxidation rate in a waste rock dump from an opencut mine. *Water Air Soil Pollut.*, 15: 405-423.

NSC [1980] - Handbook on Linear Applications. National Semiconductor Corp; Santa Clara CA. p.AN222-11.

Lowson, R.T. [1982] - Aqueous oxidation of pyrite by molecular oxygen. *Chem. Rev.* 82(5) 461-497.

Marshall, T.J. and Holmes, J.W. [1979] Measurement of water content and potential. In *Soil Physics*, Chapter 3. Cambridge University Press, Melbourne.

Peters, E. [1976] - Direct leaching of sulfides: chemistry and applications. *Metall. Trans.*, 7B: 505-517.

Timko, M.P. [1976] - A two terminal IC temperature transducer. *IEEE J. Solid-State Circuits*, SC-11 784-788.

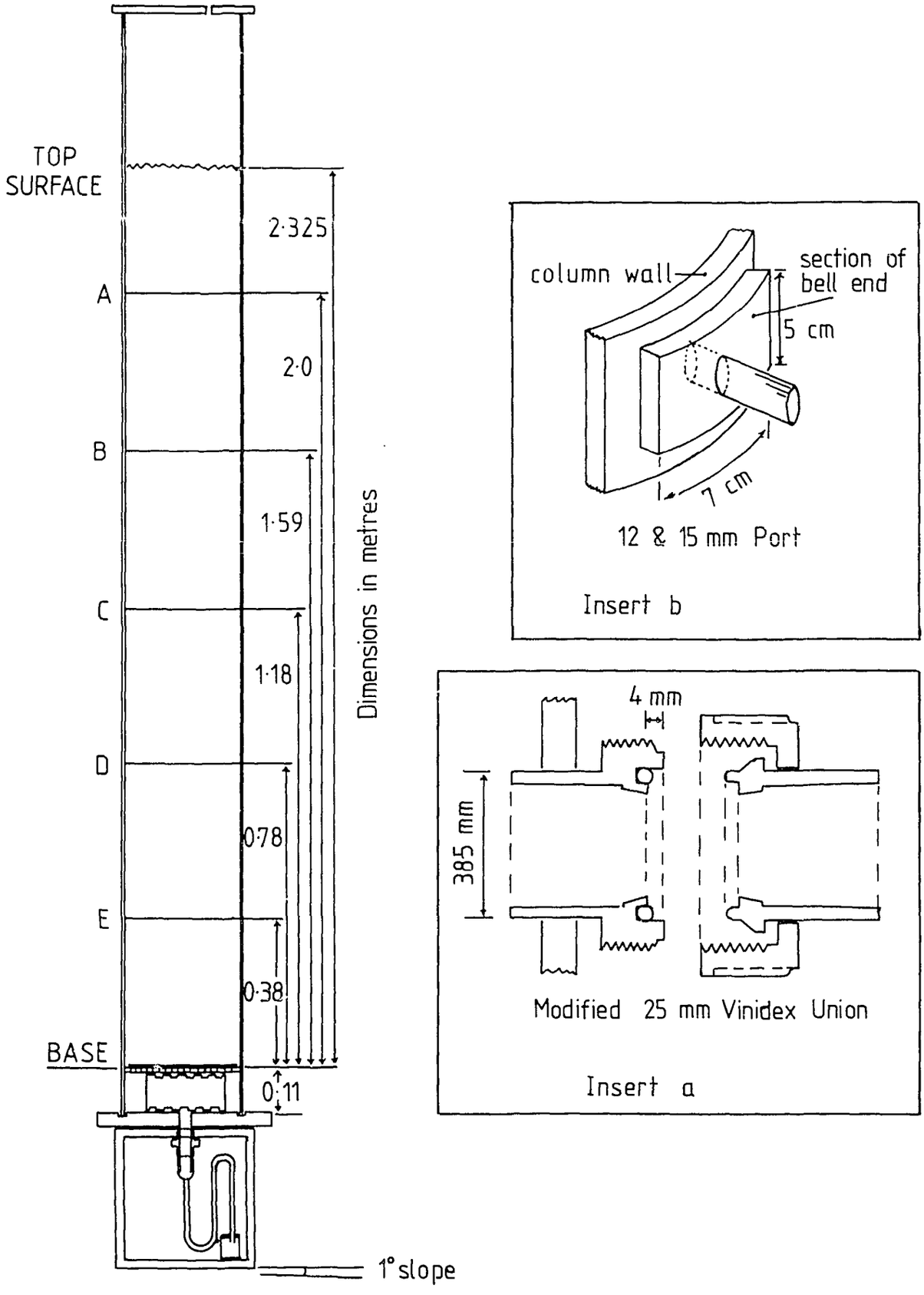

Figure 1 Scale drawing of column showing positions of ports; insert A, the 25 mm port; insert B, the 15 and 12 mm port

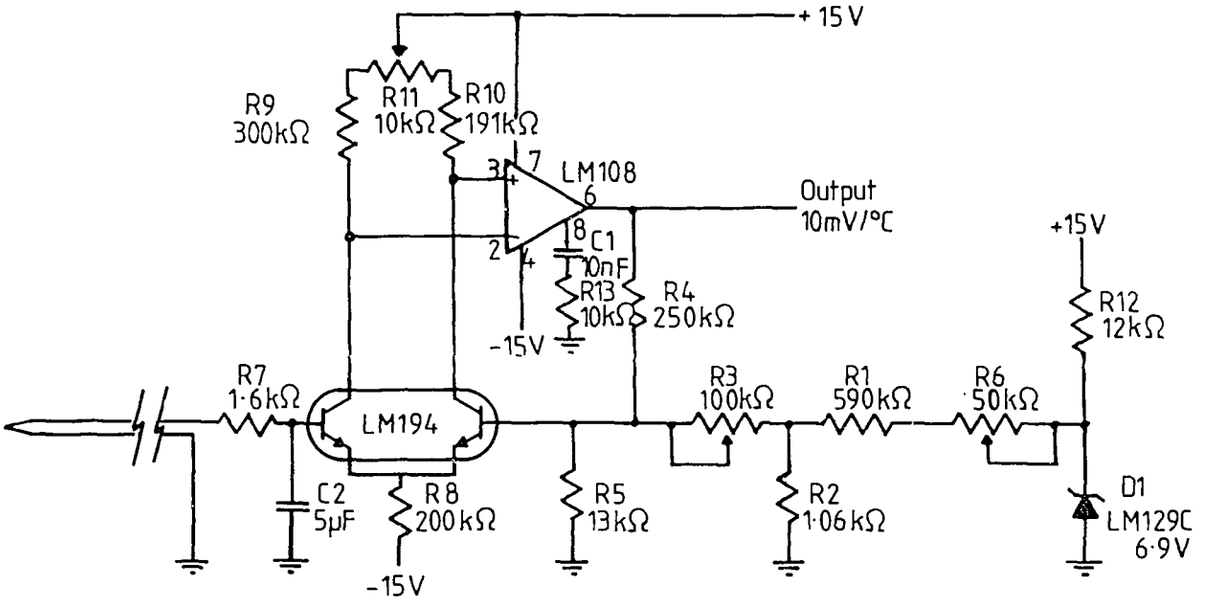

Figure 2 Thermocouple amplifier with cold junction compensation

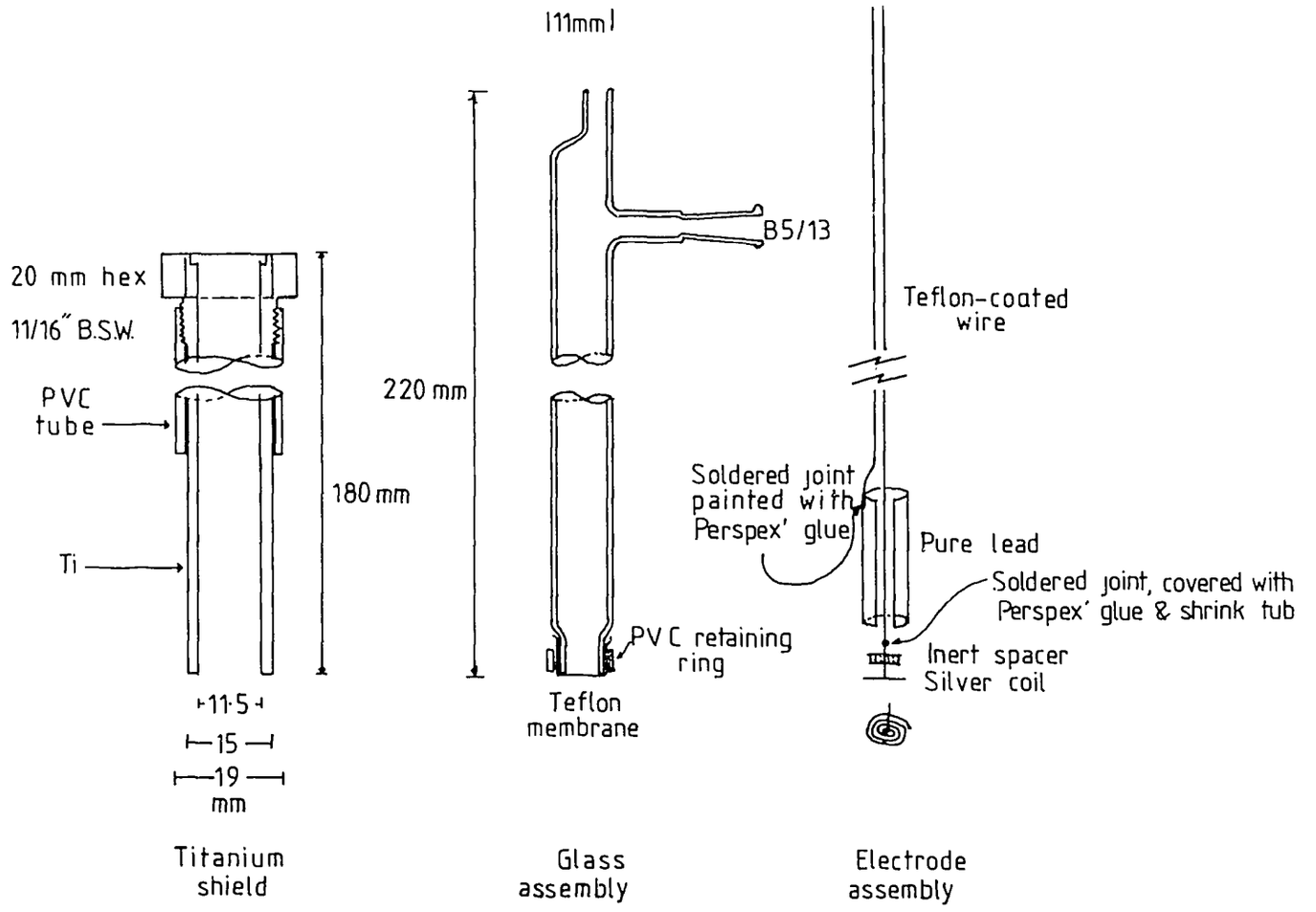

Figure 3 The oxygen probe assembly

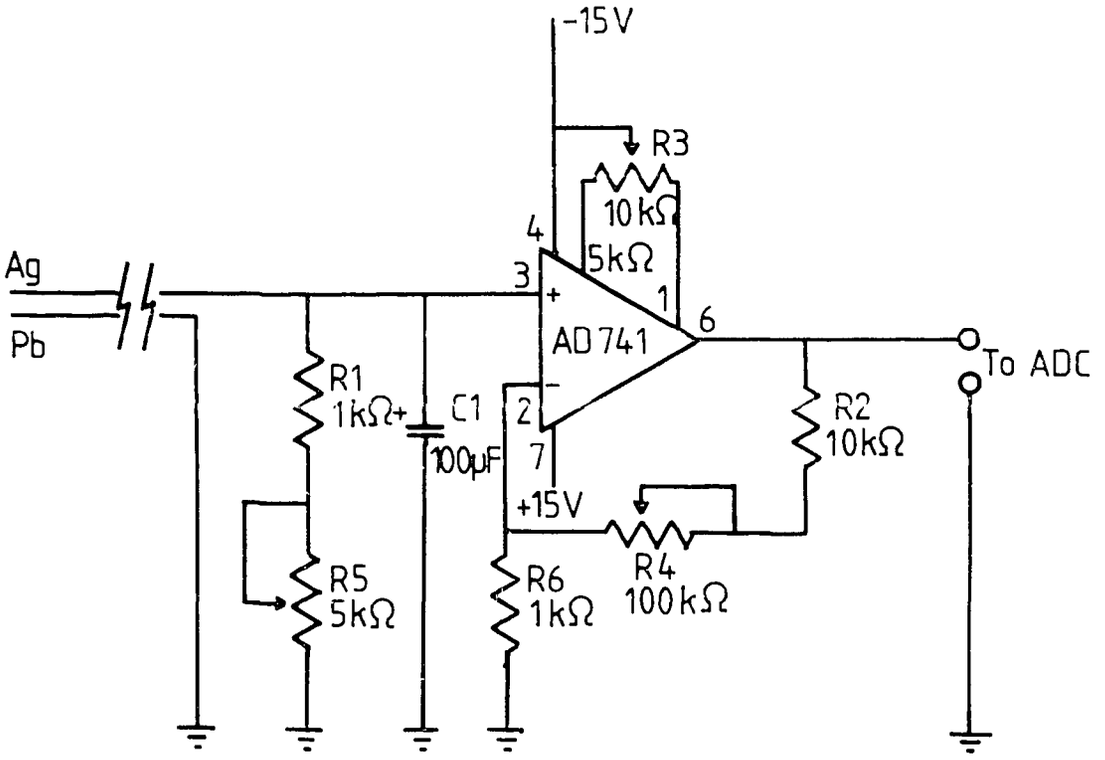

Figure 4 Oxygen probe amplifier with zero adjustment

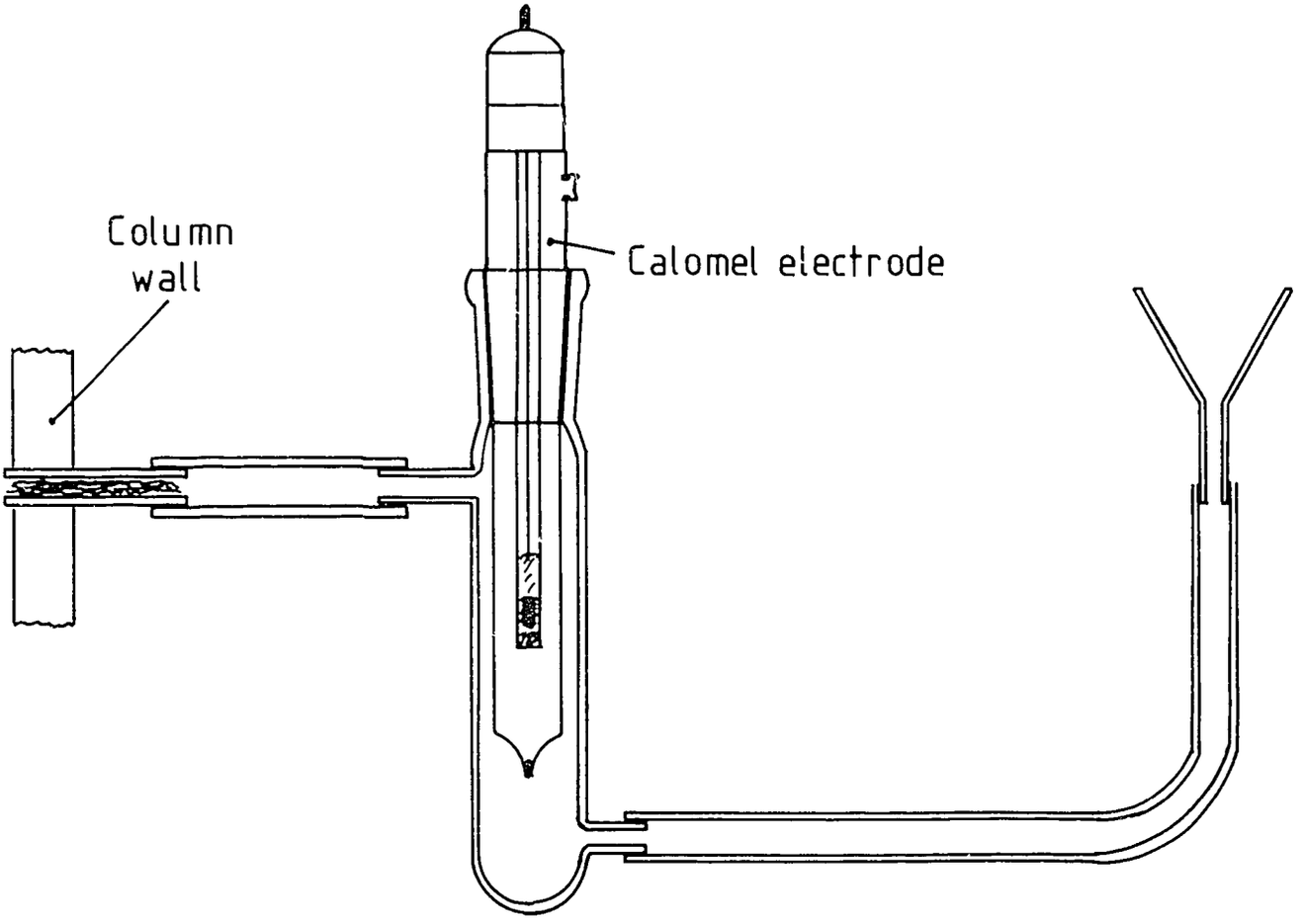

Figure 5 Redox probe reference electrode assembly

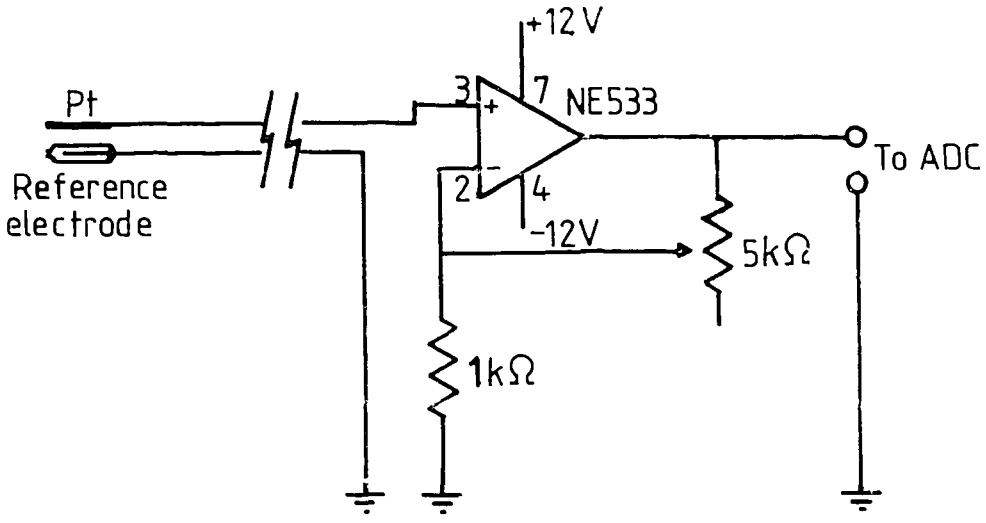

Figure 6 Redox probe amplifier

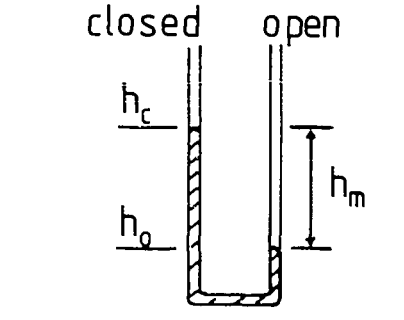

$h_m = h_o - h_c$

is - ve for suction

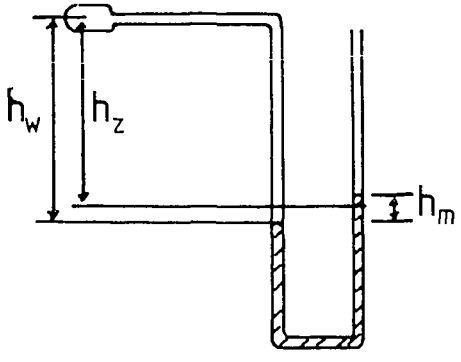

Case A h_m is +ve, h_w is +ve

$$h_h = h_m (\rho_m/\rho) - (h_z + \tfrac{1}{2} h_m)$$

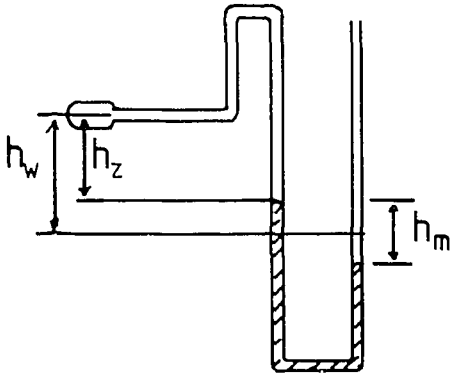

Case B h_m is - ve, h_w is + ve

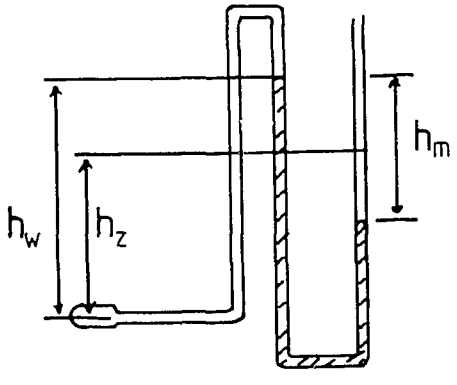

Case C h_m is - ve, h_w is - ve

Figure 7 The three cases for matric potential in an undersaturated soil. When hm is +ve and hw is -ve, then the ceramic cup must be in a saturated soil

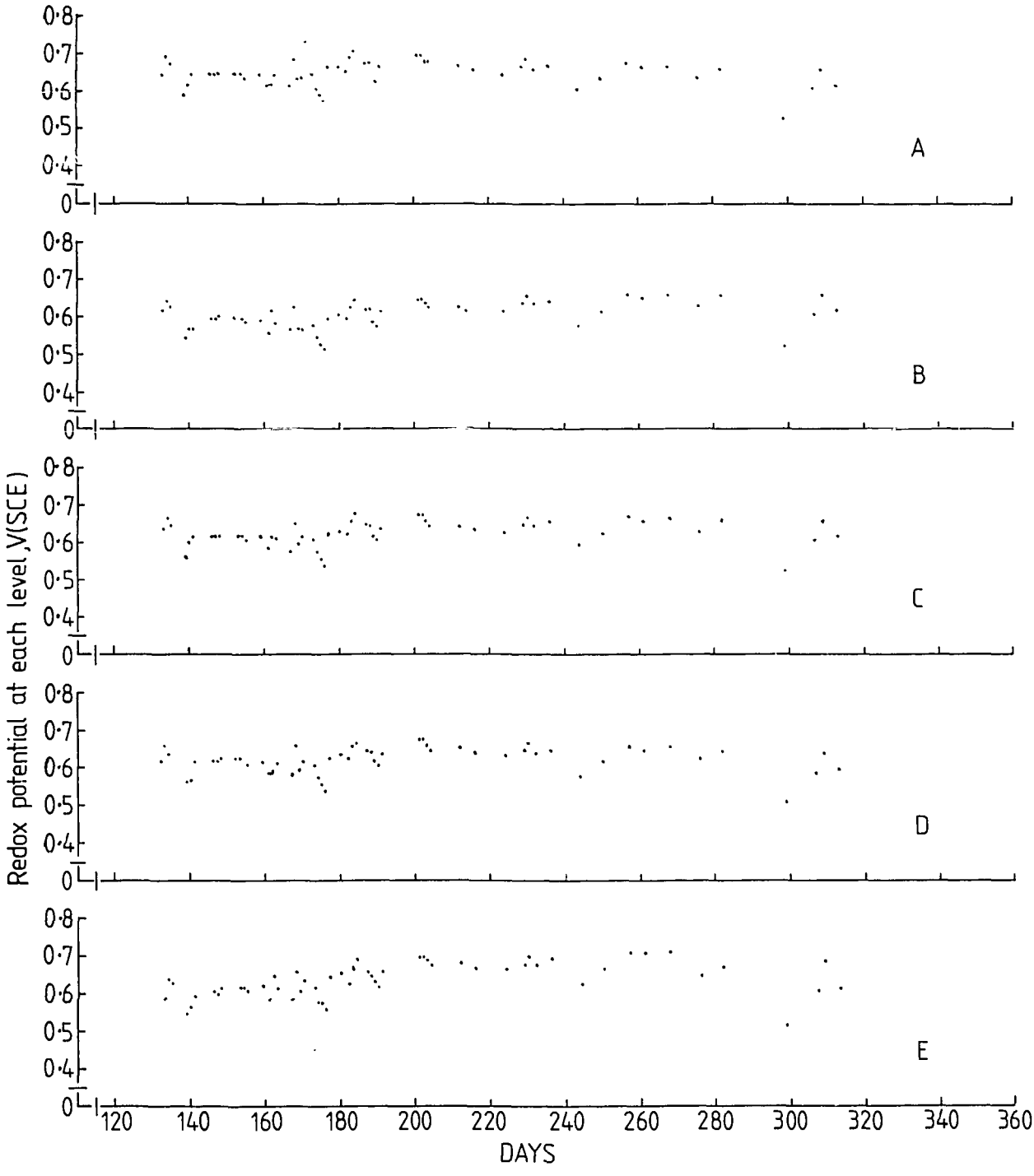

Figure 8 Plots of redox potential with reference to the saturated calomel electrode (SCE) as a function of time for the five levels

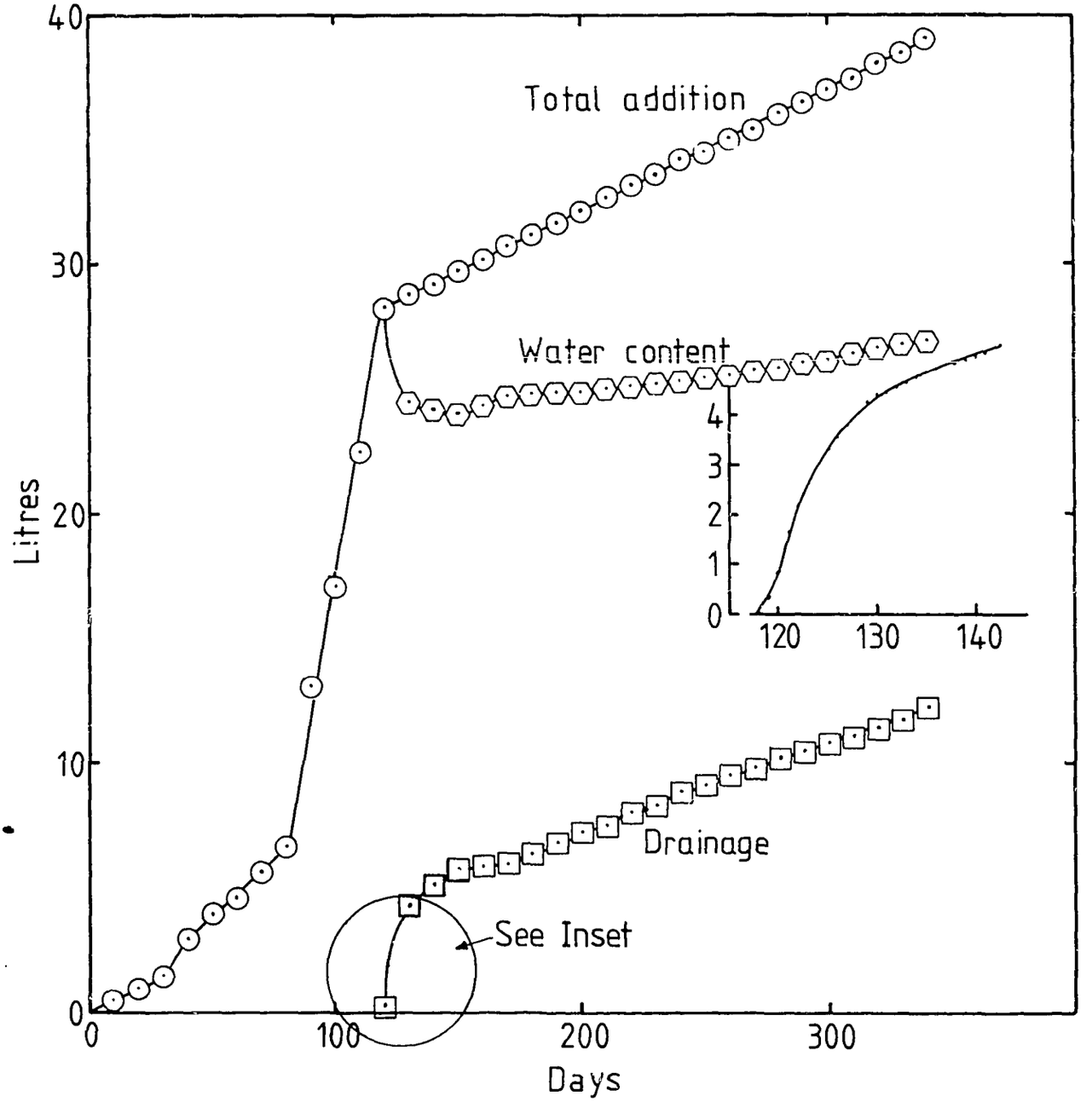

Figure 9 Plot of total water addition, water content and drainage following commissioning. The insert is a × 2 magnification of the first 25 days following the commencement of drainage

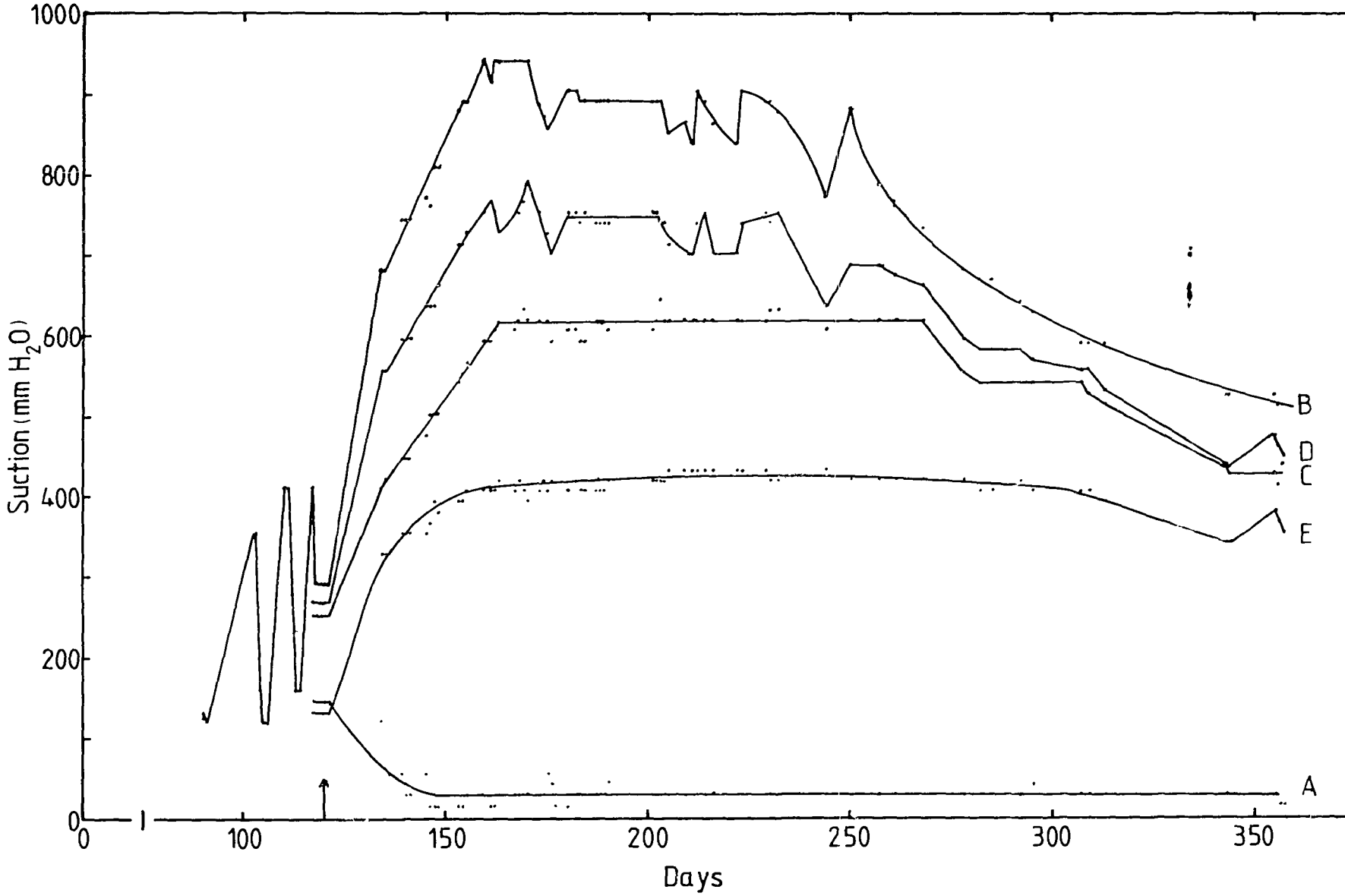

Figure 10 Plot of matric pressure at each level as a function of time. The results prior to the commencement of drainage have not been included due to the instability of the tensiometers

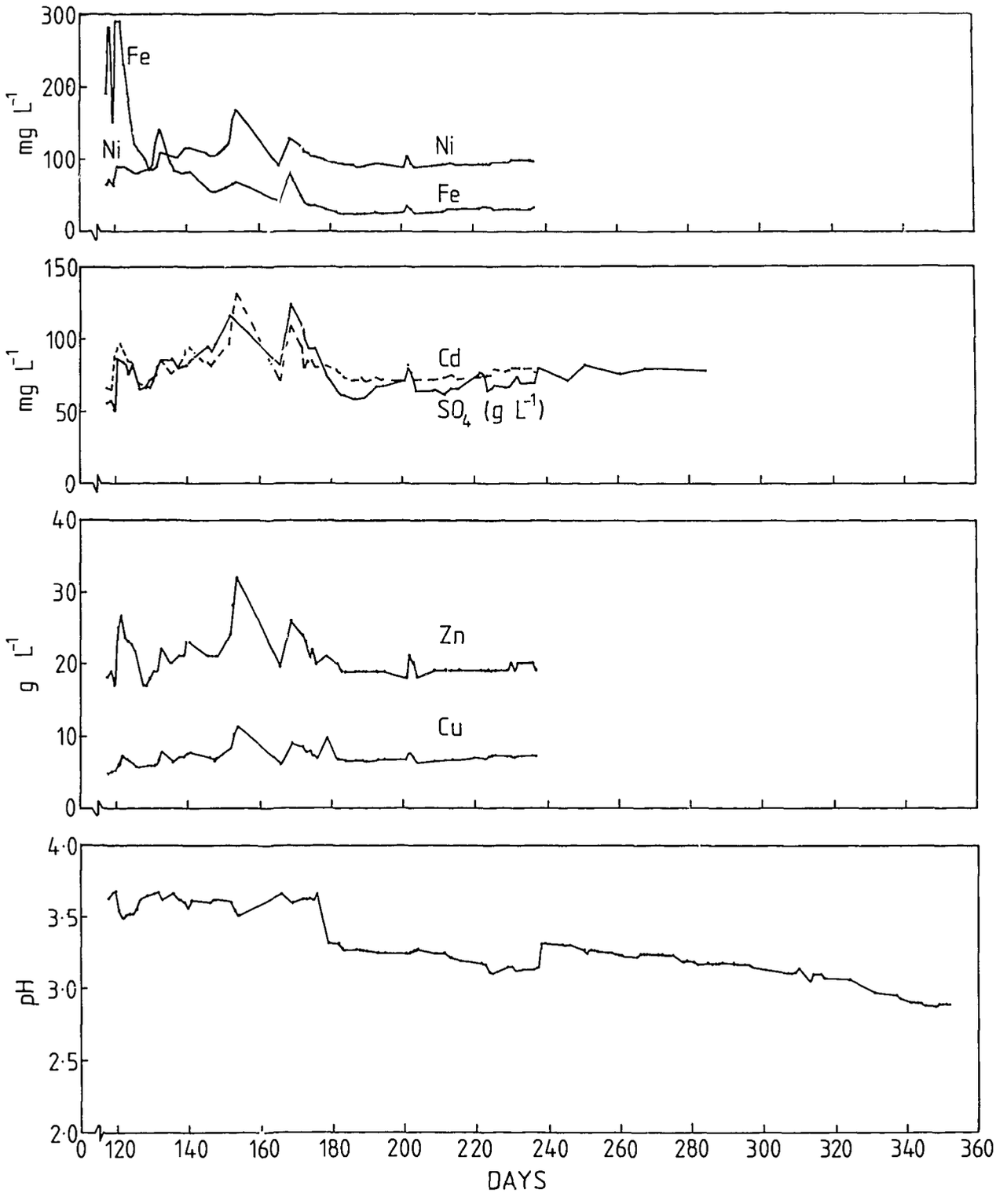

Figure 11 Plots of pH, heavy metal and sulphate concentration in the effluent as a function of time

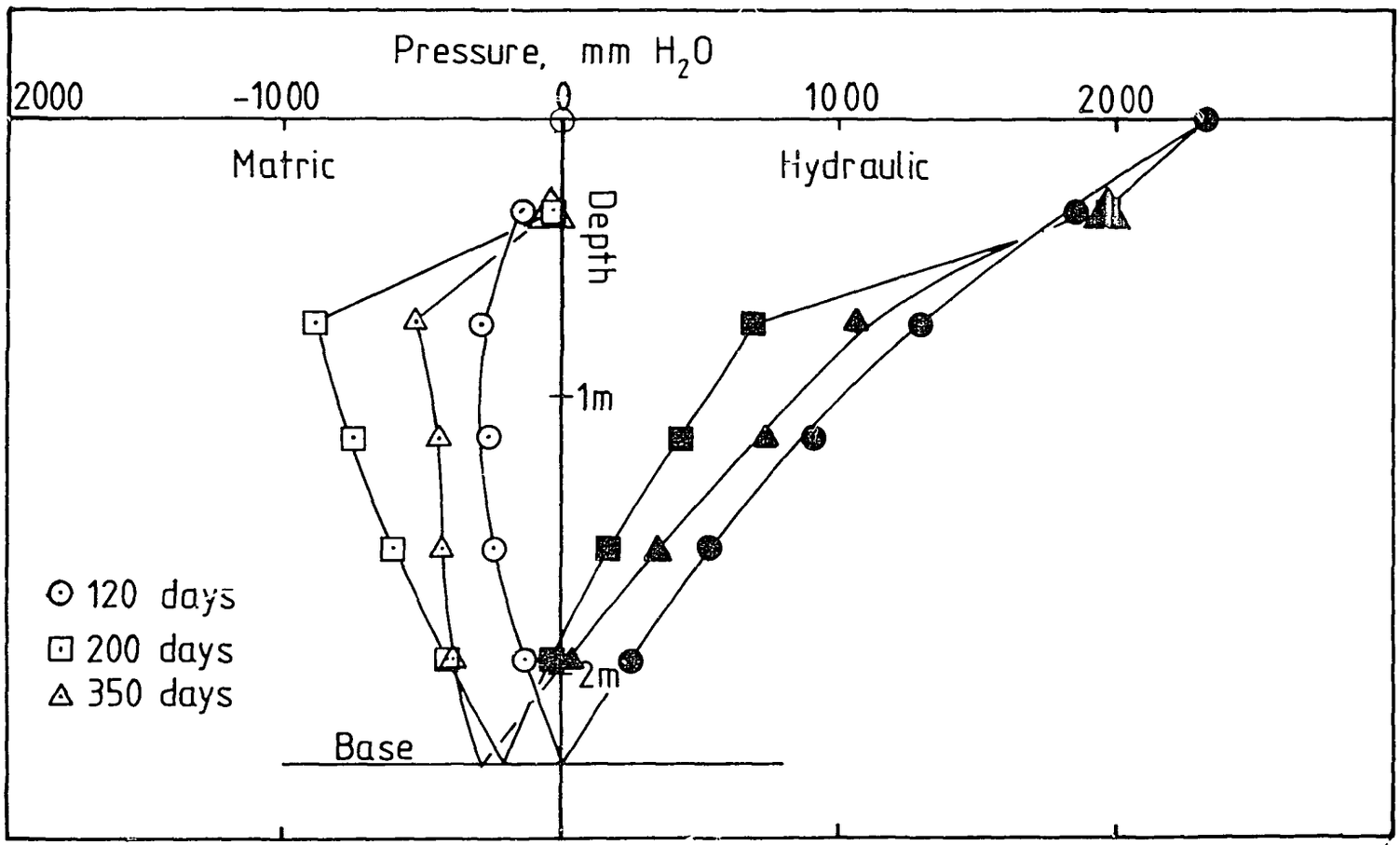

Figure 12 Plot of matric and hydraulic pressure as a function of depth for the times 120, 200 and 350 days following commissioning. The reference level was the free draining base of the column